



Nocturnal Low-level Jet Evolution in a Broad Valley Observed by Dual Doppler Lidar

THOMAS DAMIAN*, ANDREAS WIESER, KATJA TRÄUMNER, ULRICH CORSMEIER and CHRISTOPH KOTTMEIER

Institute for Meteorology and Climate Research, Karlsruhe Institute of Technology, Germany

(Manuscript received October 29, 2013; in revised form January 24, 2014; accepted January 28, 2014)

Abstract

The temporal evolution of a nocturnal low-level jet (LLJ) in the 40km broad Rhine Valley near Karlsruhe is studied, in the framework of a case study, with two heterodyne detection Doppler lidars using the new scan concept of “virtual towers”. For validation of this measuring technique, we performed comparative case studies with a tethered balloon and the highly instrumented 200m KIT tower. The findings show capabilities of the virtual tower technique for wind measurements. Virtual towers can be placed at all locations within the range of Lidar measurements. Associated with nocturnal stable stratification, the LLJ, a wind speed maximum of about 9ms^{-1} , develops at 100m to 150m agl, but the wind does not show the typical clockwise wind direction change that is reported in many other studies. This is attributed to the channeling effect occurring in broad valleys like the Rhine Valley when the boundary layer is stably stratified. Such channeling means a significant deviation of the wind direction from the Ekman spiral so that low-altitude winds turn into valley-parallel direction.

Keywords: doppler lidar, dual doppler lidar, virtual towers, wind measurement, vertical profile

1 Introduction

In general, a jet stream describes a strong wind developing when air masses with large temperature differences exist in close vicinity, for example at the polar front or in the subtropics (KRAUS, 2004). The jet can be basically explained by the thermal wind equation for geostrophic winds increasing with height. A more local phenomenon is the low-level jet (LLJ), which develops in the atmospheric boundary layer (ABL) and is caused by an inertia oscillation induced by near-ground air masses cooling after sunset. LLJs form when the wind decouples from the surface because of a strong stable stratification, and the air masses above the stable layer accelerate along the pressure gradient (BLACKADAR, 1957; STENSRUD, 1996; WANG et al., 2007). LLJs often appear at night time as demonstrated e.g., in a study by KOTTMEIER (1982), where in 10% of all nights, LLJs could be detected in an extended area over Northern Germany and the Netherlands (KOTTMEIER, 1978; KOTTMEIER et al., 1980). LLJs are important for several applications. For example, they influence the transportation of aerosols, pollutants, and trace gases (BANTA et al., 1998) and are relevant to flight safety and wind energy (EMEIS et al., 2007). BANTA et al. (2002) analyzed nocturnal LLJs systematically and characterized concerning their shear and relation to turbulence. Shear forces and turbulence cannot be neglected in atmospheric models, and a better knowledge of the char-

acteristics of LLJ may help to improve modeling of shear forces (NEWSOM and BANTA, 2003). Furthermore, wind power plants are affected by LLJs. In order to extract more wind energy, wind farms are increasingly located in complex terrain like hilly areas or forests. Especially above forest cover with respect to the forest height and the turbulence induced by forest edges (TRÄUMNER et al., 2012), hub heights have to be raised up to 150m agl. At these heights, the higher wind speeds and shear driven by LLJs have to be considered (EMEIS et al., 2007).

LLJs develop typically at heights between 100m and 300m agl and are characterized by specific wind speed and wind direction changes with height. Continuous wind data at heights between the ground and 500m agl would be highly advantageous to characterize the full extent of the LLJs for application purposes. This is difficult to obtain with in-situ measurement techniques. Only high, stationary measuring towers are able to detect LLJs with appropriate efforts. These, however, only provide data at one measurement location and are rarely available. In the last years, active remote sensing techniques have become increasingly common in wind and turbulence research. Doppler lidars are capable of providing wind measurements flexibly and with high temporal and spatial resolutions (RÖHNER and TRÄUMNER, 2013; STAWIARSKI et al., 2013; TRÄUMNER et al., 2011; TRÄUMNER et al., 2012). Doppler lidars are mostly transportable devices featuring eye-safe measurements. BANTA et al. (2002) and PICHUGINA et al. (2004) already demonstrated the successful application of Doppler lidar technology in LLJ studies.

*Corresponding author: Thomas Damian, Institute for Meteorology and Climate Research, Karlsruhe Institute of Technology, Germany, e-mail: thomas.damian@kit.edu

The dual Doppler scan technique we used for wind measurements is related to virtual towers (CALHOUN et al., 2006), and up to now has been rarely used. To implement this technique, two scanning Doppler lidars are necessary. In comparison to wind measurements using real towers or point measurements with tethered balloons or kites, virtual towers can be flexibly “positioned” even at inaccessible places like urban areas or above forests. Virtual towers can cover a vertical range from the surface up to 1.5 km agl with a vertical resolution of a few meters. It will be shown that measurements of a quality comparable to that produced by stationary towers and tethered balloons can be obtained. This emphasizes the applicability of virtual towers and the benefits of this measurement technique as demonstrated for analysis of a nocturnal LLJ as a common wind system.

2 Dual Doppler Lidar Wind Measurement

2.1 Instrument setup and virtual towers

Two powerful heterodyne detection Doppler lidar systems (WERNER, 2005) “Wind Tracer” are operated by Institute for Meteorology and Climate Research (IMK) at the Karlsruhe Institute of Technology (KIT) as an important part of the so-called KITcube (KALTHOFF et al., 2013). Both systems are able to measure radial wind velocities with a temporal resolution of 10 Hz in a range of up to twelve kilometers distance from the instrument, depending on the atmospheric conditions, such as aerosol concentration and water vapor absorption. The two instruments can perform highly synchronized scans with two-axis scanners covering the upper half-hemisphere. The technical realization of the lidar synchronization is described by STAWIARSKI et al. (2013), the lidar properties are given in Table 1. This study is based on a field experiment where both systems were operated in a synchronized scan mode similar to the stop-and-stare method (DRECHSEL et al., 2010, also called “step-and-stare”). Both lidar beams were directed towards a point in space where they measure the line-of-sight wind velocity during a defined period of time (Fig. 1). Afterwards, they move on to the next intersecting point located vertically above, repeating the measurement. This scan mode enables the construction of so-called “virtual towers” (CALHOUN et al., 2006). At each height level we collected data for two seconds. Because the scanner needs some time to accelerate and decelerate, the time needed for one iteration of stop-and-stare at all 16 height levels is about one minute. In a time period of ten minutes, we have collected data for approximately twenty seconds per level. In this work, we used a height profile with a higher resolution at lower altitudes and a lower resolution at higher altitudes. All in all, we measured wind speed and direction at 16 heights at 20 m, 50 m, 75 m, 100 m, 150 m, 200 m, 250 m, 300 m, 500 m,

Table 1: Properties of the lidar systems WTX and HYB.

	WTX	HYB
wave length in nm	1.617	2.023
laser type	Er:YAG	TM:LuAG
pulse length in ns	300	370
pulse energy in MJ	2.7	2.0
pulse frequency in Hz	750	500
sampling rate in MHz	250	250
north coordinate	N 49° 7' 6.528"	N 49° 7' 33.096"
east coordinate	E 8° 15' 3.002"	E 8° 14' 39.095"

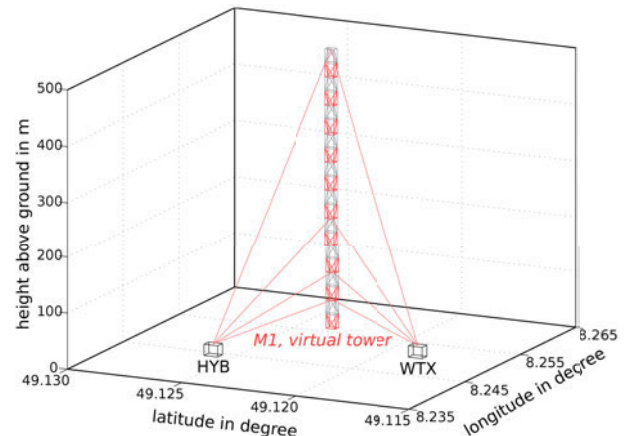


Figure 1: Scheme of wind measurements at a virtual tower executed by two lidar systems (WTX, HYB) using stop-and-stare methods.

750 m, 1000 m, 1500 m, 2000 m, 2500 m, 3000 m agl. Due to the low aerosol concentration, at height levels above 1500 m agl we could not detect useful data. It is advisable to adjust the total measuring height precisely to the research intention. In general, there are two possibilities to use the virtual tower method. Using the stop-and-stare method as we did is advantageous when a special vertical resolution is desired and measurements at high altitudes have to be conducted. The scanner movement between two points can be operated very fast with scan velocities up to 20° s^{-1} . The second possibility is based on continuous RHI scans (CALHOUN et al., 2006). Here, the lidar’s elevation is varied at a constant azimuth. Due to a constant scan velocity around 5° s^{-1} this scan method gets very time-consuming when scanning high altitude differences.

The virtual tower method is well-suited to analyze local wind phenomena such as LLJ. In fact, by measuring the horizontal wind vectors at different heights, we are able to analyze local wind phenomena. Compared to other studies e.g., by BANTA et al. (2002) where the lidar measures in RHI mode in wind direction, our scan method is not dependent on frequent wind direction measurements to guarantee that the lidar points in wind direction. Furthermore, the method we used is better at detecting wind shear for the same reason that we have data which is independent on wind direction. On

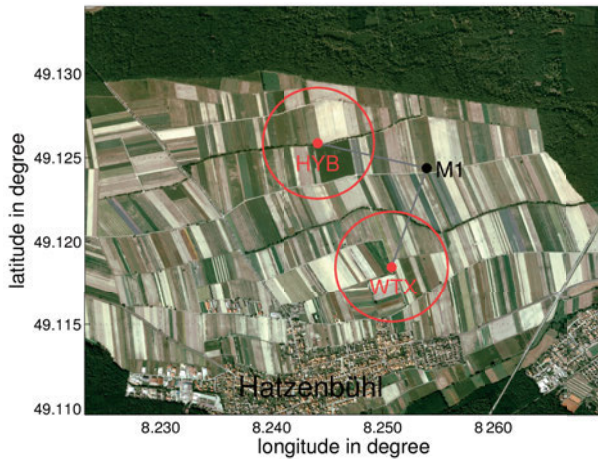


Figure 2: Positions of the lidar systems (WTX and HYB, coloured red) and the virtual tower (M1, black) near Hatzenbühl, Germany. Useful dual Doppler results everywhere outside the red circles. (Picture: Geocontent GmbH)

the other hand, the method BANTA et al. (2002) used in their work is less time-consuming and can be performed with one Doppler lidar.

$$v_{r_i} = \begin{pmatrix} u \\ v \\ w \end{pmatrix} \cdot \begin{pmatrix} \cos \varphi_i \cdot \sin \alpha_i \\ \cos \varphi_i \cdot \cos \alpha_i \\ \sin \varphi_i \end{pmatrix} \quad (2.1)$$

Based on the line-of-sight velocities v_{r_i} (Eq. (2.1)) from both lidars and under the necessary requirement that the average vertical wind velocity $\bar{w} = 0$, the west-easterly wind component (u) and the south-northerly wind component (v) can be determined:

$$\bar{u} = \frac{\bar{v}_{r_1} \cos \varphi_2 \cos \alpha_2 - \bar{v}_{r_2} \cos \varphi_1 \cos \alpha_1}{\cos \varphi_1 \cos \varphi_2 \sin(\alpha_1 - \alpha_2)} \quad (2.2)$$

$$\bar{v} = -\frac{\bar{v}_{r_1} \cos \varphi_2 \sin \alpha_2 - \bar{v}_{r_2} \cos \varphi_1 \sin \alpha_1}{\cos \varphi_1 \cos \varphi_2 \sin(\alpha_1 - \alpha_2)} \quad (2.3)$$

The azimuth angles are described by α_i , the elevation angles by φ_i . In this work, we used a ten-minute average time, therefore turbulence measurements are not possible. Depending on the elevation angle, respectively measuring height, a prevailing vertical wind causes an linear dependent inaccuracy in horizontal wind vector data. To quantify this inaccuracy, we expect $\bar{w} \neq 0$ in Eq. (2.1). Fig. 2 shows the inaccuracy of the horizontal wind vector Δv as a function of measuring height, respectively elevation angle. The values $|\bar{w}| = 0.5 \text{ m s}^{-1}$, $|\bar{w}| = 1.0 \text{ m s}^{-1}$, $|\bar{w}| = 1.5 \text{ m s}^{-1}$ fit for most meteorological situations and give an overview of, how precise measurements can be. At low vertical wind speeds ($|\bar{w}| \leq 0.5 \text{ m s}^{-1}$), the inaccuracy $\Delta v \leq 1.5 \text{ m s}^{-1}$ is acceptable, even at heights of 1.5 km agl. When the vertical wind $|\bar{w}| \geq 1.0 \text{ m s}^{-1}$, the measuring accuracy at high altitudes decreases significantly ($\Delta v \geq 4.0 \text{ m s}^{-1}$). This is

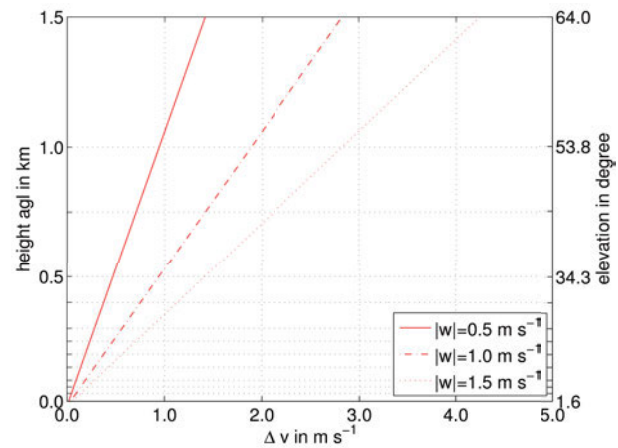


Figure 3: Impact of prevailing vertical wind speed $|w|$ in horizontal wind vector v measurement depending on measuring height in m agl, respectively elevation angle in degree at location M1.

caused by the high elevation angles, used in this work. When the virtual tower $M1$ is positioned in a greater distance to both lidar systems, it is possible to measure at same heights using lower elevation angles, so the impact of vertical wind speed is weaker. Nevertheless, at low altitudes ($\leq 0.5 \text{ km agl}$), the accuracy is acceptable ($\Delta v \leq 1.5 \text{ m s}^{-1}$) even under moderate convective conditions with vertical wind speeds up to 1.5 m s^{-1} .

To guarantee a good data quality, we filtered all data by considering the signal-to-noise ratio (SNR). The SNR can be used as a measure to distinguish useful data from the background noise. The threshold SNR value has to be chosen with specific regard to the device. For our lidar systems, we used a rather conservative setting where much data got filtered and the SNR had to be $\geq -6 \text{ dB}$.

For the first comparative measurements, both lidars were located at KIT Campus North (KIT CN) in January 2011. The instruments were set up approximately 400 m away from each other and 1.5 km away from the 200 m high KIT tower. During this comparison, both lidars measured in fixed stare mode, i.e. the lidars' azimuth (elevation) angles are fixed at $\alpha_1 = 196.6^\circ$ ($\varphi_1 = 3.9^\circ$) and $\alpha_2 = 213.55^\circ$ ($\varphi_2 = 4.25^\circ$), respectively. The crossing point of the laser beams was located near the tower next to a sonic anemometer at a height of 100 m with an intersecting angle of 16.95° . The optimal settings for dual Doppler measurements are given at an intersecting angle of 90° (STAWIARSKI et al., 2013, Eq. 23). Due to signal noise of the lidar instruments, which causes an error in radial velocity of about $\Delta r_v = 0.15 \text{ m s}^{-1}$ the dual Doppler lidar signal also shows an error. This can be quantified to a combined error for the west-easterly wind component u and the south-northerly wind component v and yields to $\Delta u + \Delta v \approx 0.73 \text{ m s}^{-1}$ (intersecting angle: 16.95°). The sonic anemometer (GILL, SOLENT R2) has a measurement frequency of 20 Hz and a precision of $\pm 0.1 \text{ m s}^{-1}$.

In summer 2011, both instruments were moved to a field site near Hatzenbühl, approximately 13 km away from KIT. Fig. 2 shows the positions of both lidars and the virtual tower in the north of Hatzenbühl. The site in Hatzenbühl was chosen because of the flat landscape and a straight forest edge (TRÄUMNER et al., 2012) lying in its north, making it suitable for a study of airflow over forest edges. The position of the virtual tower ($M1$) was selected because of a nearly perpendicular angle of 84.7° between both beams, giving optimal geometrical conditions for dual Doppler lidar measurements. With $\Delta u + \Delta v \approx 0.21 \text{ m s}^{-1}$ the lidars' error is low in comparison to the set-up used at KIT Campus North.

2.2 Setup of tethered-balloon probe

For tethered-balloon in-situ measurements, an IMK-developed probe was attached to the balloon by a trapeze mounting system which allows the probe to adjust to the wind field using a rear rudder. The balloon is about 6 m long at a diameter of 1.25 m and is filled with helium. Using an electrical winch, the whole system is securely fixed to the ground and can be adjusted to different heights. A radio telemetry transmits the data to the ground with a time resolution of about 2.6 s.

The probe measures several meteorological variables such as wind speed and direction, temperature, dew point, and air pressure. Wind measurements are carried out by a vane anemometer and a compass unit. Measuring height is derived from air pressure measurements. The balloon was raised at the virtual tower position $M1$ in Fig. 2.

By calibrating the probe in a wind tunnel using a DWD (Deutscher Wetterdienst) calibrated propeller anemometer (Meteolabor, ONZ, precision: $\pm 0.1 \text{ m s}^{-1}$), we can ensure a sufficient data quality. During 75 minutes, the tunnel air speed was raised stepwise between $0.3 \text{ m s}^{-1} \leq v_{\text{tunnel}} \leq 5.0 \text{ m s}^{-1}$. By fitting a linear regression, we can derive the calibration function in equation (2.4) which was used for the following data analysis and provides an accuracy of approximately $\pm 0.1 \text{ m s}^{-1}$.

$$f(x) = 0.0546x + 0.1798 \quad (2.4)$$

3 Comparative Measurements

3.1 Comparison with meteorological tower

Comparative measurements between remote sensing lidar systems and in-situ systems like ultra-sonic anemometers or probes at tethered balloons have to consider the different measurement characteristics of the techniques. The comparison of single values in a time series will fail due to beam averaging effects of the lidars, inertia effects of anemometers (balloon), and slightly different measurement locations. For this reason, we used averaged time series in the following.

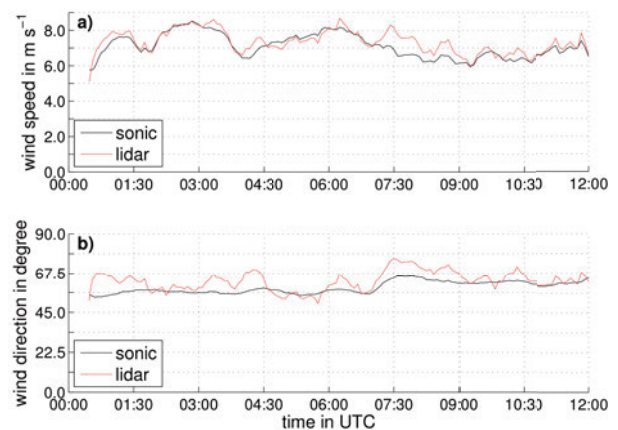


Figure 4: 30 min moving average values of a) the wind speed and b) the wind direction obtained from in-situ tower measurements and remote dual Doppler lidar measurements. Data acquisition of 28th of January, 2011, 00:00 UTC to 12:00 UTC.

For the comparative case study with the ultra-sonic anemometer, a 12 h period on 28th of January, 2011 was chosen. The measured radial wind components $r_{v,HYB}$ and $r_{v,WTX}$ at the crossing point near the anemometer were converted into the west-east wind component u as well as the south-north component v using Eqs. (2.2) and (2.3). Afterwards, all time series were averaged by a moving average (averaging time 30 min, time step 5 min). Fig. 4 shows the results for the corresponding wind speed and wind direction.

A comparison of the in-beam direction velocities measured by the two lidars and the corresponding components from the in-situ measurements shows linear correlation coefficients of the WTX system with 0.98 and 0.96 for the HYB system. The root mean squared deviation for the WTX system is 0.16 m s^{-1} , respectively 0.31 m s^{-1} for the HYB system. It is noticeable that the dual Doppler signal is less flattened than the towers' signal. We assume that the measurement set-up we conducted in this case study is responsible for this effect. According to an acute intersecting angle of both lidar beams (16.95°), the setting is not optimal for dual Doppler measurements (see also section 2.1).

The correlation coefficients for the wind direction is 0.64 and for the wind speed 0.86. The root-mean-squared deviation between the in-situ and the dual Doppler values is 5.9° and 0.42 m s^{-1} respectively. A more detailed look at the correlation is given in Figs. 5, a) and b). With respect to measurements which are not independent from the sensor design (WIESER et al., 2001), the performance of the two lidars is satisfying.

3.2 Comparison with tethered-balloon probe

The second case study was performed between 12:20 UTC and 13:50 UTC on 21st of October, 2011. Wind data at two different height levels were measured simultaneously by the dual Doppler lidar system and the tethered balloon. Between 12:20 UTC and 13:10 UTC,

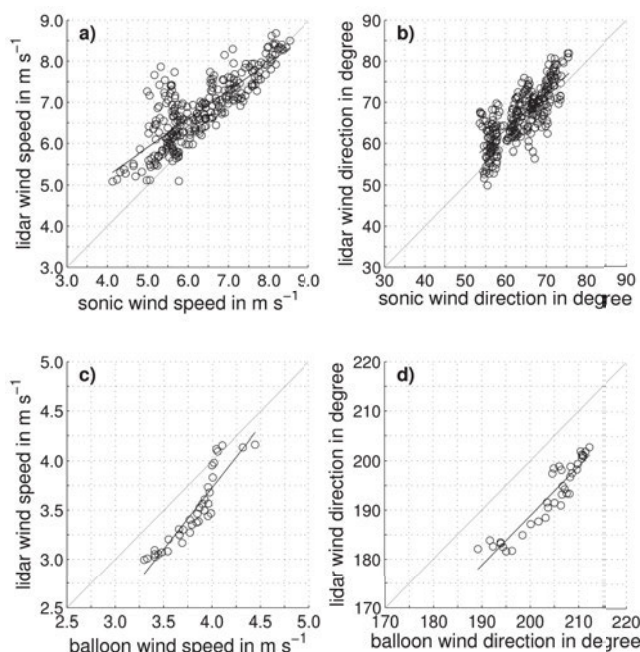


Figure 5: Correlations of wind speed (a and c) and wind direction (b and d) measured by lidar, ultrasonic anemometer, and tethered balloon are shown. Points depict the pairs of values, the black line represents the fit through the values. The gray line is the angle bisector. Sonic data acquisition of 28th of January, 2011, 00:00 UTC to 12:00 UTC and tethered-balloon data acquisition of 21st of October, 2011, 12:20 UTC to 13:50 UTC.

we detected wind speed and direction in 50m agl, between 13:10 UTC and 13:50 UTC in 100m agl. The meteorological situation on 21st of October, 2011 was characterized by a high-pressure system with weak pressure gradients. Fig. 6, a) shows the heights where dual Doppler lidar measurements took place and the tethered-balloon measuring height. While dual Doppler lidar measurement data correspond to a fixed height, the tethered balloon was pending around this height as a result of its own motion in the wind. At the beginning of the measurements, both systems collected data at different heights due to adjusting problems. The balloon measured wind data 10.5m (average over the whole time: 3.1 m) below the dual Doppler lidar.

Moving averages of wind speed (Moving average (150 seconds averaging period) for both measuring systems show good accordance (Fig. 6, b)). Only around 12:45 UTC and 13:45 UTC, the measured wind speeds differ significantly. The average deviation in wind speed is 0.2ms^{-1} while the maximum deviation is about 0.75ms^{-1} . The wind speed data show a root-mean-squared deviation of 0.2ms^{-1} . Over the whole period of time, the wind direction measured is very similar (Fig. 6, b)). Maximum differences of about 15.4° can be seen around 12:45 UTC, 12:55 UTC and 13:40. The data show a bias of 11.2° where balloon data are shifted clockwise. Root-mean-squared deviation is calculated to 2.5° .

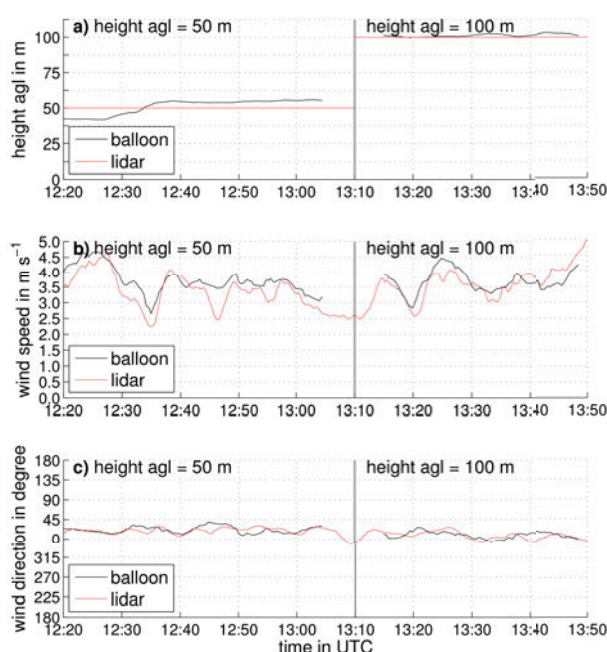


Figure 6: Moving average (150s averaging time) of a) measuring height, b) the wind speed, and c) the wind direction obtained from tethered-balloon and remote dual Doppler lidar measurements. Data acquisition of 21st of October, 2011, 12:20 UTC to 13:50 UTC.

For a more exact interpretation of the wind speed, we take a look at the correlation in Fig. 5, c). All points are concentrated near the bisector angle and the fit is biased with 0.4ms^{-1} . The results concerning wind direction are slightly different (Fig. 5, d)). Wind direction is biased with 11.2° where the balloon measures greater angles. These differences may be caused by impreciseness of the compass unit of the tethered-balloon probe. In contrast, the correlation of values around the fit is quite accurate. By calculating the linear correlation coefficient for both wind speed and direction, we can quantify the correlation. With $r_{\text{speed}} = 0.92$ and $r_{\text{direction}} = 0.93$, we are satisfied with the measuring quality of our dual Doppler lidar system and the scan method.

4 Nocturnal Low-level Jet Evolution

The LLJ case study was performed during the night of 19th to 20th of September, 2011. The weather situation was influenced by a high-pressure system located over southern Germany. Hence, in Hatzenbühl, there were winds from northwesterly direction. The wind speed was between 0ms^{-1} and 9ms^{-1} .

Time series of wind speed and wind direction between 19th of September, 2011, 11:00 UTC and 21st of September, 2011, 03:00 UTC at eight heights between 20m and 300m agl are shown in Fig. 7. In the first seven hours, the wind calmed down at all heights from about 5ms^{-1} near zero. Due to the low wind speeds, the wind direction varied considerably between 270° and 360° during this time.

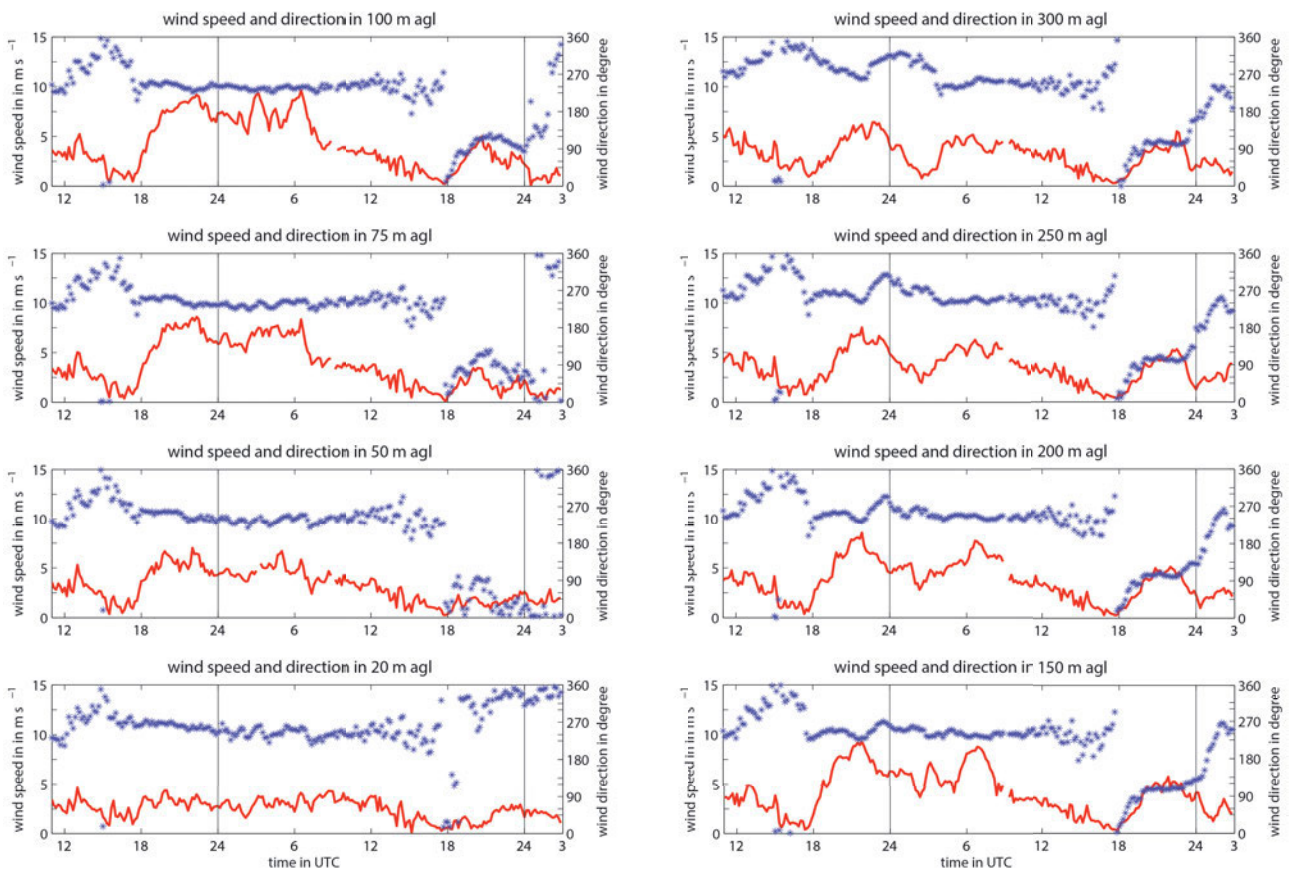


Figure 7: Virtual tower showing time series of wind speed (red curve) and wind direction (blue stars) at eight measuring heights between 20 m and 300 m agl in the time window of 19th of September, 2011, 11:00 UTC to 21st of September, 2011, 03:00 UTC.

In the evening of 19th of September, 2011 from about 18:00 UTC to 21:00 UTC, a strong increase in wind speed to maximum values of about 9 m s^{-1} at a height of 100 m agl could be observed. This strong winds ceased with sunrise on 20th of September 2011, 7:00 UTC. The increase in wind speed in the evening could be detected at all heights from 50 m to 250 m agl. In 20 m agl the wind speed was constant at around 2.5 m s^{-1} . At 300 m agl, a maximum wind speed of about 5 m s^{-1} was measured showing only a weak increase at night. At all measuring heights above 150 m agl, a local minimum in wind speed was observed above the LLJ maximum at 3:00 UTC. The wind apparently showed a predominant direction of 270° at nearly all heights over the entire night.

Wind speed decreased in the morning at all heights between 75 m and 200 m agl. From 20th of September, 2011, 12:00 UTC to 18:00 UTC, the wind speed calmed down to values near zero analogue to the previous day.

Data from the 200 m tower at KIT Campus North was used to characterize the stability of the lower atmosphere. In Fig. 8, the vertical profiles of temperature are shown for different times on 19th and 20th of September, 2011. While at daytime, the stratification was nearly neutral (Fig. 8 a); 15:00 UTC, 17:00 UTC and 18:00 UTC) or even lightly unstable (11:00 UTC), the stratification stabilized signifi-

cantly between 18:00 UTC and 19:00 UTC, which is in agreement with sunset around 17:30 UTC. Between 2:00 UTC and 8:00 UTC, the stratification was stable, from 09:10 UTC to 12:00 UTC the stratification was neutral, while at 14:00 UTC, we had unstable conditions again. Sunrise took place around 07:00 UTC. A comparison of Fig. 7 and Fig. 8 shows a relationship between the increase, respectively decrease of wind speed and stabilization (around 19th of October 2013, 18:00 UTC), respectively labilization (around 20th of October, 2013, 08:00 UTC) of the air masses. The vertical profiles of horizontal wind speed measured with dual Doppler lidar at different times are shown in Fig. 9. At 19th of September, 2011, between 11:00 UTC and 22:00 UTC the atmosphere got stably stratified (Fig. 9, a)), while labilization took place at 20th of September, 2011, between 2:00 UTC and 14:00 UTC (Fig. 9, b)). Above 300 m height agl, wind speed shows an equivalent behavior for both situations with values between 5 m s^{-1} and 8 m s^{-1} . At all times when the prevailing stratification was stable, we found a LLJ in the vertical wind speed profiles. The LLJ is located between 50 m and 300 m agl with maximum wind speed of about 9 m s^{-1} which is in total agreement with other studies like BANTA et al., (2002). The vertical profiles of wind direction are displayed in Fig. 10. In the evening of 19th of September, 2011 (Fig. 10, a)) the wind direction at heights above

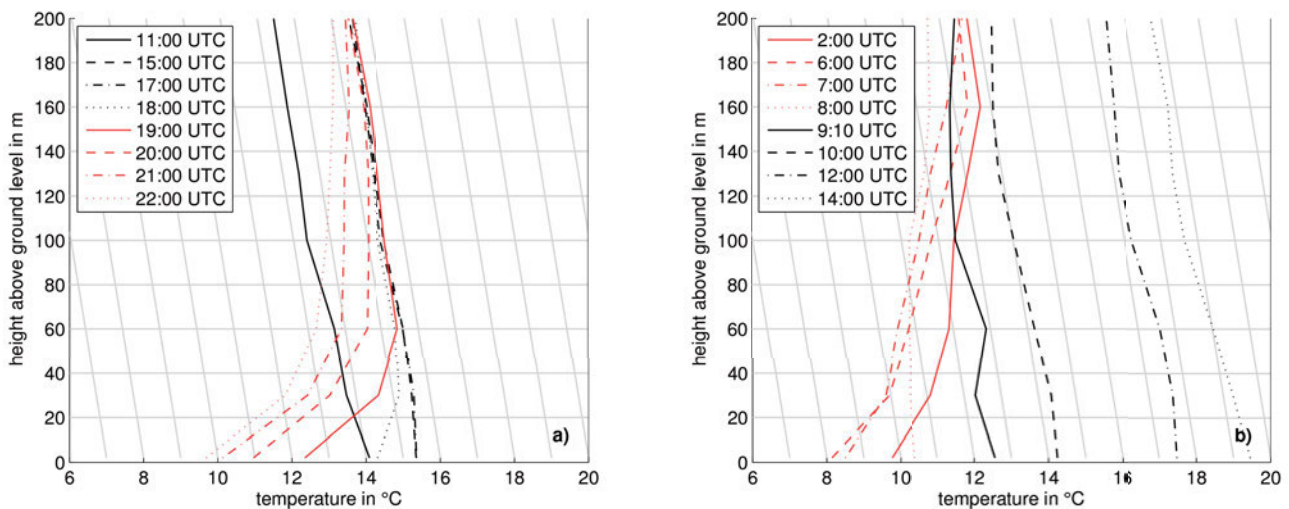


Figure 8: Vertical profiles of air temperature measured at the 200m tower at the KIT Campus North at different times between 19th of September, 2011, 11:00 UTC and 20th of September, 2011, 14:00 UTC. The gray solid lines depict the dry adiabatic lapse rate for comparison to the prevailing stratification. a) shows the ABL stabilization while b) shows the ABL labilization.

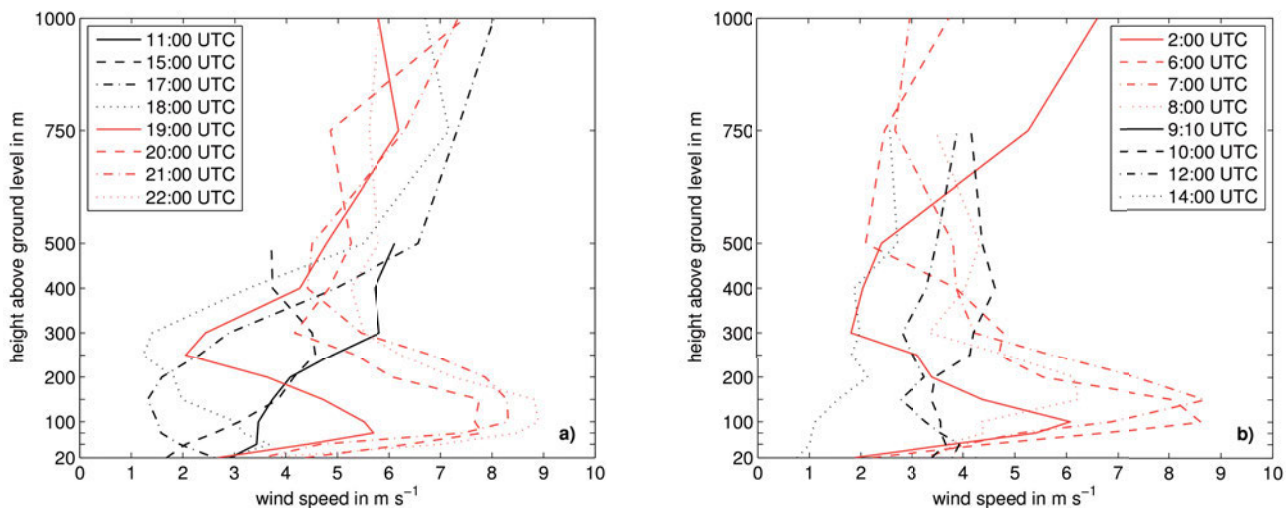


Figure 9: Vertical profiles of wind speed measured with dual Doppler lidar from 19th of September, 2011, 11:00 UTC to 20th of September, 2011, 14:00 UTC at the position of the virtual tower *M1* in Hatzenbühl. a) shows the ABL stabilization while b) shows the ABL labilization.

400m agl is between 270° and 335° at all times. At height levels below 400m agl, for most of the time, the wind is turned to wind directions 225° and 270°. This shift is not caused by a nocturnal LLJ as it should be theoretically. A LLJ-caused wind shift typically is a clockwise time-dependent change in wind direction as reported in many other studies (BLACKADAR, 1957; STENSRUD, 1996). Because Hatzenbühl is located in the 40km broad Rhine Valley, the wind at lower height levels is affected by a channeling effect. In the work by VOGEL (1987), the wind flow in the Rhine Valley was simulated and it could be shown that the wind field in the Rhine valley is affected by channeling effects. KALTHOFF and VOGEL (1992) analyzed the channeling effect in the Rhine Valley using the 200m KIT tower data over a period of 16 years. They found that in 96% of all events with channeling effects, the atmosphere was

stably stratified. Additionally, in 66% of all channeling events, the wind speed was less than 3 ms⁻¹ at 40m agl. Also, in the situation analyzed in this work, the wind direction at heights below 300m agl turned parallel to the Rhine Valley, which mainly results in effective wind directions at lower height levels of about 230°. These conclusions are in agreement with the results in Fig. 4.

As we have two phenomena appearing due to stable stratification, the nocturnal LLJ and the channeling effect, the vertical profiles of wind speed and wind direction (Fig. 9 and Fig. 10) are influenced in a different way. As the wind speed shows a distinct tendency to higher values of about 9 ms⁻¹ at height levels between 50m and 300m agl caused by the LLJ, the wind direction is not affected by the LLJ but shows a wind shift at height levels below 400m agl due to the channeling effect of the Rhine Valley.

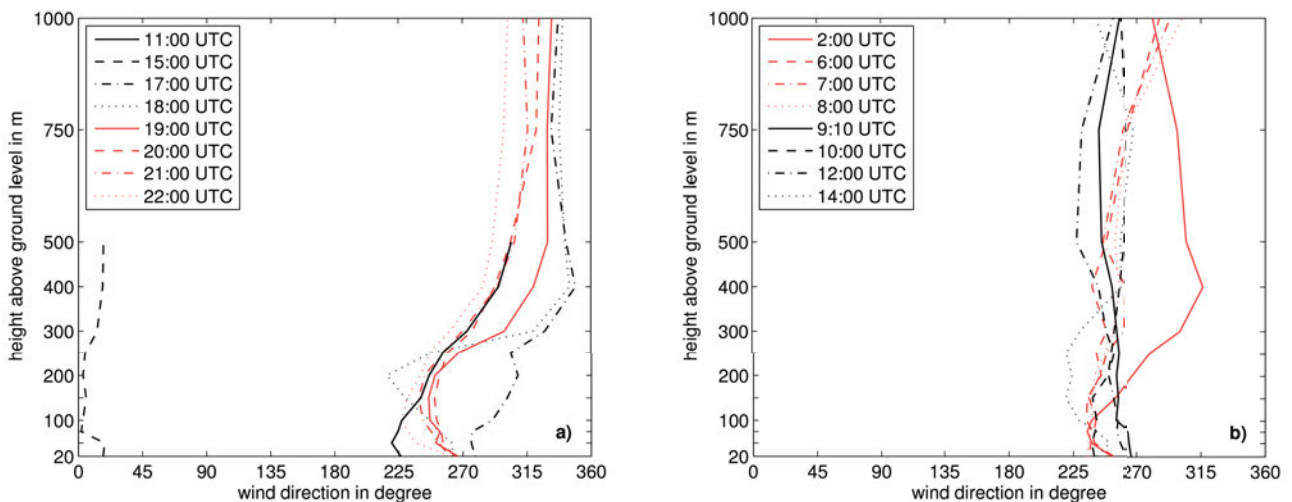


Figure 10: Vertical profiles of wind direction measured with dual Doppler lidar from 19th of September, 2011, 11:00 UTC to 20th of September, 2011, 14:00 UTC at the position of the virtual tower *M1* in Hatzenbühl. a) shows the ABL stabilization while b) shows the ABL labilization.

5 Conclusions

In this study, we analyzed the evaluation of a nocturnal low level jet (LLJ) using dual Doppler lidar. With measurements along a virtual tower, an up to now rarely used scan technique, we can calculate the vertical profile of the horizontal wind vector. The study demonstrates the potential of the virtual tower measuring technique and shows in a case study how a nocturnal LLJ can be investigated properly. A comparison with data from a stationary tower and a tethered balloon shows the reliability of the virtual tower measurement technique.

Deploying two Doppler lidars in a dual Doppler mode provides highly synchronized measurements of two radial wind velocity components. Applying a scan strategy with sufficiently low elevation angles gives the opportunity to compute the horizontal wind vector. By measuring winds at different heights over a fixed position, vertical profiles of horizontal winds, so-called “virtual towers” can be derived.

Using virtual towers for wind measurements in combination with temperature measurements from the stationary meteorological KIT tower, a nocturnal LLJ can be detected and characterized. Our data shows the development of a nocturnal LLJ causing a maximum in wind speed of about 9 m s^{-1} at heights between 50 m and 300 m agl. The LLJ occurs during stable stratification. Because of a channeling effect in the Rhine Valley, the expected wind shift caused by the LLJ is suppressed. Instead, we can see a turning of wind direction from about 40° to 60° at lower height levels to a wind direction parallel to the 40 km broad Rhine Valley.

Using dual Doppler lidar methods, we can measure common local wind systems like the LLJ or the channeling effect and additionally detect the flow at higher levels up to 1.5 km agl. We can interpret the wind shear in the whole ABL which provides a benefit compared

to real towers. With this additional knowledge, it is possible to investigate common ABL wind systems more thoroughly. An other advantage of the application of a dual Doppler setup and the virtual towers is the flexibility of the measurements, because the towers can simply be placed at any location of interest in the lidars’ surrounding area. There are numerous possibilities for measurements over complex terrain. For example, this system can be used above forests and water surfaces, in street canyons and urban surroundings, and on airports. Regarding this, it is feasible to investigate the impact of orography, forests, and buildings on the existing wind situation and thus helps to understand how the flow and existing obstacles interact. This information can be very useful to researchers in wind power plant subject areas.

The KIT lidar systems are installed on swap bodies which make them mobile. Additionally, it is possible to construct more than one virtual tower in a line or any other arbitrary alignment to investigate and characterize the horizontal effects of complex terrain on the wind field.

References

- BANTA, R., C. SENFF, A. WHITE, M. TRAINER, R. MCNIDER, R. VALENTE, S. MAYOR, R. ALVAREZ, R. HARDESTY, D. PARRISH, OTHERS, 1998: Daytime buildup and nighttime transport of urban ozone in the boundary layer during a stagnation episode. – *J. Geophys. Res.* **103**, 22–519.
- BANTA, R., R. NEWSOM, J. LUNDQUIST, Y. PICHUGINA, R. COULTER, L. MAHRT, 2002: Nocturnal low-level jet characteristics over Kansas during CASES-99. – *Bound.-Layer Meteor.* **105**, 221–252.
- BLACKADAR, A., 1957: Boundary layer wind maxima and their significance for growth of nocturnal inversions. – *Bull. Amer. Meteor. Soc.* **38**, 283–290.
- CALHOUN, R., R. HEAP, M. PRINCEVAC, R. NEWSOM, H. FERNANDO, D. LIGON, 2006: Virtual towers using coherent Doppler lidar during the Joint Urban 2003 dispersion experiment. – *J. Appl. Meteor. Climatol.* **45**, 1116–1126.

- DRECHSEL, S., G. J. MAYR, M. CHONG, F. K. CHOW, 2010: Volume scanning strategies for 3D wind retrieval from dual-Doppler lidar measurements. – *J. Atmos. Oceanic Technol.* **27**, 1881–1892.
- EMEIS, S., M. HARRIS, R. M. BANTA, 2007: Boundary-layer anemometry by optical remote sensing for wind energy applications. – *Meteorol. Z.* **16**, 337–347.
- KALTHOFF, N., B. VOGEL, 1992: Counter-current and channelling effect under stable stratification in the area of Karlsruhe. – *Theor. Appl. Climatol.* **45**, 113–126.
- KALTHOFF, N., B. ADLER, A. WIESER, M. KOHLER, K. TRÄUMNER, J. HANDWERKER, U. CORSMEIER, S. KHODAYAR, D. LAMBERT, A. KOPMANN, N. KUNKA, G. DICK, M. RAMATSCHI, J. WICKERT, C. KOTTMEIER, 2013: KITcube – a mobile observation platform for convection studies deployed during HYMEX. – *Meteorol. Z.* **22**, 633–648.
- KOTTMEIER, C., 1978: Trajektorien unter Einfluß eines nächtlichen Grenzschichtstrahlstroms. – *Meteorol. Rundschau* **31**, 129–133.
- KOTTMEIER, C., 1982: Die Vertikalstruktur nächtlicher Grenzschichtstrahlströme, Dissertation. – Im Selbstverlag des Instituts für Meteorologie und Klimatologie der Universität Hannover, 132 pp.
- KOTTMEIER, C., D. LEGE, R. ROTH, 1980: Ein Messsystem zur Sondierung der planetarischen Grenzschicht. – *Meteorol. Rundsch.* **33**, 9–13.
- KRAUS, H., 2004: Die Atmosphäre der Erde: Eine Einführung in die Meteorologie. – Springer Berlin Heidelberg New York, 422 pp.
- NEWSOM, R.K., R. M. BANTA, 2003: Shear-flow instability in the stable nocturnal boundary layer as observed by Doppler lidar during CASES-99. – *J. Atmos. Sci.* **60**, 16–33.
- PICHUGINA, Y., R. BANTA, N. KELLEY, S. SANDBERG, J. MACHOL, W. BREWER, 2004: Nocturnal low-level jet characteristics over southern Colorado. – In: Preprints, 16th Symp. on Boundary Layers and Turbulence, Portland, ME, American Meteorological Society, CD-ROM, Volume 4.
- RÖHNER, L., K. TRÄUMNER, 2013: Aspects of Convective Boundary Layer Turbulence Measured by a Dual-Doppler Lidar System. – *J. Atmos. Oceanic Technol.* **30**, 2132–2142.
- STAWIARSKI, C., K. TRÄUMNER, C. KNIGGE, R. CALHOUN, 2013: Scopes and Challenges of Dual-Doppler Lidar Wind Measurements – An Error Analysis. – *J. Atmos. Oceanic Technol.* **30**, 2044–2062.
- STENSRUD, D. J., 1996: Importance of low-level jets to climate: A review. – *J. Climate* **9**, 1698–1711.
- TRÄUMNER, K., C. KOTTMEIER, U. CORSMEIER, A. WIESER, 2011: Convective boundary-layer entrainment: short review and progress using doppler lidar. – *Bound.-Layer Meteor.* **141**, 369–391.
- TRÄUMNER, K., A. WIESER, B. RUCK, C. FRANK, L. RÖHNER, C. KOTTMEIER, 2012: The suitability of Doppler lidar for characterizing the wind field above forest edges. – *Forestry* **85**, 399–412.
- VOGEL, B., 1987: Numerische Untersuchungen zur Kanalisierung der Luftströmungen in Tälern. – Dissertation, Inst.f. Met TH Darmstadt, 136 pp.
- WANG, Y., C. KLIPP, D. GARVEY, D. LIGON, C. WILLIAMSON, S. CHANG, R. NEWSOM, R. CALHOUN, 2007: Nocturnal low-level-jet-dominated atmospheric boundary layer observed by a Doppler lidar over Oklahoma City during JU2003. – *J. Appl. Meteor. Climatol.* **46**, 2098–2109.
- WERNER, C., 2005: Doppler Wind Lidar. – In: C. WEITKAMP (Ed.): Lidar. – Springer Series in Optical Sciences Vol. **102**, 325–354.
- WIESER, A., F. FIELDER, C. CORSMEIER, 2001: The influence of the sensor design on wind measurements with sonic anemometer systems. – *J. Atmos. Oceanic Technol.* **18**, 1585–1608.